Eur J Cancer, Vol. 26, No. 3, pp. 241–251, 1990.
Printed in Great Britain

0277-5379/90$3.00 + 0.00

Influence of Hormono- and/or Chemotherapy on the MXT Mouse Mammary Tumor as Monitored by ^{31}P MRS

CHRISTIAN SCHEIBER,* ROBERT KISS,†§ YVAN DE LAUNOIT,†‖ PAUL SIJENS‡ and JANOS FRÜHLING*

**Department of Radiotherapy and Nuclear Medicine, Institut J. Bordet, Free University of Brussels, 1 rue Héger-Bordet, 1000 Brussels, Belgium, †Laboratory of Histology, Faculty of Medicine, Free University Brussels, 2 rue Evers, 1000 Brussels, Belgium and ‡Department of Radiotherapy, University Hospital, Catharijnesingel 101, Utrecht, The Netherlands*

Abstract—*We describe the early* in vivo *modifications that occurred in the MXT mouse hormone sensitive mammary tumor following various treatments which were monitored by ^{31}P NMR spectroscopy. The MXT mouse mammary tumor was subjected to clinically relevant low-dose chemotherapy, i.e. seven cycles of* 20 mg/kg *cyclophosphamide (CPA) with or without an attempt at estrogenic cell recruitment prior to the CPA treatment. NMR measurements were begun at the end of the CPA treatment in order to evaluate the remaining 'long-term' chemotherapy-induced modifications within the MXT tumors. Statistical analyses performed on the ^{31}P NMR parameters revealed that treatment had induced significant effects on bATP/PCr, Pi/PCr and PME/PDE only, with PCr being the most discriminating index. Its presence within MXT tumors was verified by means of an analysis of perchloric extracts. The results indicate a relative decrease of PME/PDE and a better conservation of PCr within the CPA-treated group as compared to the control one. This feature appeared even prior to any macroscopic modifications, as was the case within the group which contained tumors smaller than* 120 mm^2, *and where no significant differences appeared between the mean sizes of the MXT cancers. In contrast, within the G2 group, which contained tumors equal to or larger than* 120 mm^2, *CPA significantly slowed down tumor growth, while the administration of estradiol (E2) prior to CPA treatment antagonized the positive CPA-induced therapeutic effect. In conclusion, the non-invasive follow-up of the chemotherapeutic treatment of a clinically relevant mammary tumor model by ^{31}P NMR spectroscopy backed up by statistical analyses revealed metabolic changes that appeared well before any modifications in histopathology or growth.*

INTRODUCTION

THE GROWTH of breast cancer has long been known to be influenced by hormones, and this property was used in therapeutic schemes almost a century ago [1]. Since then, numerous new modalities of systemic therapy have become available: initially used for palliative purposes in cases of overt metastatic dissemination or in inoperable cases, chemotherapy and/or hormonal treatments are now given at earlier stages in the hope of preventing recurrences in patients running high risks of relapse [2]. On the basis of biochemical studies [3, 4], most clinicians now decide to treat breast cancers by hormono- or chemotherapy according to the ER and PgR amounts in such tumors [2, 5–11].

Many experimental murine models have been used to obtain a better understanding of breast cancer biology (for review see [12]). Among them, the MXT neoplasm is a model used by Clark and co-workers to demonstrate sensitivity to estrogens [13, 14] and progestins [15]. We have also shown

Accepted 24 October 1989.
§R.K. is 'Chargé de Recherche au Fonds National de la Recherche Scientifique' (F.N.R.S), 5 rue d'Egmont, 1050 Brussels, Belgium.
‖Y. de L. is the holder of a grant from the 'Institut pour l'encouragement de la Recherche Scientifique dans l'Industrie et l'Agriculture' (IRSIA), 6 rue de Crayer, 1050 Brussels, Belgium.
Correspondence to Professor J. Frühling, M.D., Ph.D.
Abbreviations: CPA: cyclophosphamide; DPG: day post tumor grafting; E2: 17-beta-estradiol; ER: estrogen receptors; G6P: glucose-6-phosphate; GPC: glycerophosphorylcholine; GPE: glycerophosphorylethanolamine; NAD: nicotinamide; NMR: nuclear magnetic resonance; NTP: nucleoside triphosphate; ORG-2058: organon 2058; PC: phosphorylcholine; PCr: phosphocreatine; PDE: phosphodiesters; PE: phosphorylethanolamine; Pi: inorganic phosphate; PgR: progesterone receptors; PME: phosphomonoesters; MRS: magnetic resonance spectroscopy.

that cancer growth is influenced by estradiol [16–18], progesterone [19, 20], prolactin [21] or gonadoliberin [22]. Furthermore, an estrogenic cell recruitment performed on an MXT tumor may, in some cases, significantly improve its sensitivity to cyclophosphamide (CPA) treatment [23, 24].

The present studies were undertaken to determine early changes, i.e. those that occur prior to any macroscopic modifications in an MXT mouse mammary tumor submitted to clinically relevant low-dose chemotherapy (CPA treatment) with and without an attempt at estrogenic cell recruitment for the purpose of inducing a possibly E2–CPA co-operativity (see [23, 24]). In a previous study, we had already monitored the CPA- and/or E2-induced effect by ^{31}P NMR [25] that allows a non-invasive evaluation of tumor metabolism through the semi-quantitative analysis of mobile high-energy phosphates and phospholipid precursors. This methodology had previously been used in various experimental tumor models [26, 27].

Tumor growth and steroid hormone receptor measurements were also conducted.

MATERIALS AND METHODS

1. *Chemicals*

Estradiol-17-beta (E2) and cyclophosphamide (CPA) were purchased from Sigma Chemicals Co (St Louis, MO) and Farmitalia Carlo Erba (Belgium) respectively. All the solutions used for administration were prepared at the time by appropriate dilution with sterile saline (9.0 g NaCl/l).

Tritiated estradiol (spec. act.: 100 Ci/mmol) and tritiated ORG-2058 (spec. act.: 50 Ci/mmol) were purchased from the Radiochemical Centre (Amersham, U.K.).

2. *Animals and tumor transplantation procedure*

The original MXT mammary tumor of the C57BL × DBA 2f/F1 (B6D2F1) mouse strain is a transplantable subcutaneous model initially developed by Watson *et al.* [13] on a urethane-treated female carrying a pituitary isograft under the renal capsule. The passage used here for the transplantation procedure displayed the feature of a poorly differentiated adenocarcinoma and was identical (histopathology, ER content, growth pattern) to those of the MXT BOG.I T25-T30 strain previously described [28]. The tumor was maintained in our laboratory by regular transfers performed monthly on female B6D2F1 mice aged between 8 and 12 weeks (21–23 g; Iffa-Credo, Lyon, France). For the present experiment, 10 tumors were selected of about 1 cm^3 each and without visible areas of necrosis. These tumors were pooled and minced under sterile conditions into standardized 10 mm^3 pieces. Two fragments, one on each flank, were inoculated subcutaneously through a trochar (ga. 13) into 30 10-week-old female mice.

3. *Experimental schedule*

The mice were housed in three groups defined as OO (10 mice), OO + CPA (10 mice) and OO + E2 + CPA (10 mice): all the animals were ovariectomized 15 days after the tumor graft in order to eliminate the endogeneous production of sexual steroids.

The OO + CPA animals received seven i.p. injections of 20 mg/kg every 2 days from the 15th day post-graft (DPG) to the 27th DPG; the OO+ E2 + CPA mice received seven 2-day treatments according to the following schedule: 0.25 μg E2 i.p. followed 24 h later by 20 mg/kg CPA from the 15th DPG. This schedule was chosen on the basis of previous experiments that showed a positive estradiol–cyclophosphamide co-operativity [23, 24]. In the present case we used E2 pulses (see [24]) instead of continuous E2 stimulation (see [23]) for convenience of NMR monitoring.

NMR measurements were performed every 3 days from the 23rd day post-graft to the 43rd day post-graft.

4. ^{31}P *NMR spectroscopy*

a. In vitro. *In vitro* spectroscopy was performed at 4.7 T by means of a 200 MSL spectrometer (Bruker, A.G. Karlsruhe, F.R.G.) on material extracted according to the methodology previously described [29] following the suggestions of Evanochko *et al.* [30]. The neutralized extract was measured in the presence of 100 mM EDTA and 20% D_2O. The following acquisition parameters were used: 60°C flip angle, 8 k data points, 2048 scans and 0.819 recycle time. A 3 Hz line broadening filter was applied before Fourier transformation. The chemical shifts in the phosphorus resonances were referenced to internal glycerophosphorylcholine for both *in vitro* and *in vivo* spectra. The main resonance assignments were carried out on the basis of data recorded in the literature [30].

b. In vivo. Proton-coupled ^{31}P high resolution spectra were obtained with the same 200 MSL spectrometer (Bruker AG, Karlsruhe, F.R.G.) equipped with imaging facilities and coupled to a vertical 150-mm bore 4.7 T supraconducting magnet.

The typical acquisition parameters corresponding to a mean 60° flip angle were as follows: 30 μs pulse length, 5 kHz spectral width, 4 k data points, 90 ms acquisition time, 3 s delay time and 600 transients, all of which were coherently averaged using the cyclops phase cycling pulse programme

('cyclops'). Free induction decay was zero-filled once to 4 k, and an exponential multiplication (25 Hz line broadening) was applied before the Fourier transformation.

The mice were anesthetized with a single i.p. injection (0.15 ml) of a chloral hydrate solution (7 mg/l of saline) which maintained anesthesia for 45 min. Preliminary experiments using sequential administrations of chloralhydrate revealed that this anesthesia procedure did not alter the metabolites of the tumors. The skin overlaying the tumor was shaved before the NMR assessments. The animals were positioned in a plastic holder with the tumor centered directly beneath the 10 mm diameter solenoidal coil. The home-built probe included a copper Faraday shield to prevent extraneous signals from the surrounding muscle tissues [26, 31]. The probe was designed in such a manner that its sensitive volume was in the homogeneous region of the main field. The coil was tuned to 81 MHz and 1H external double tuning circuitry was used for shimming purposes [32].

The chemical shifts of the phosphorus resonances were referenced to internal glycerophosphocreatine (GPC). After phase and baseline corrections, the relative peak areas were determined through the use of a curve analysis program (Bruker, Belgium). This program assumed a Lorentzian resonance lineshape.

5. *NMR data presentation*

Taking into account the differing spin-lattice (1/T1) relaxation times of the various ^{31}P compounds, the results relative to metabolites were presented as ratios so as to decrease any errors that might occur with absolute values. Although acquisition parameters were chosen in order to obtain an adequate signal-to-noise ratio within the 30 min acquisition time without any relative detectable saturation effect, the data still presented partially relaxed Fourier transformed spectra.

6. *Tumor growth measurements*

Tumor size was measured every three days by means of a caliper and expressed as 'area' (mm^2) by multiplying together the two largest diameters.

7. *Validation of NMR measurements*

The same probe was used for each tumor, regardless of size. Preliminary experiments ascertained that the relative saturation factors remained invariant with regard to tumor size and treatment, thereby offering valid comparisons between changing metabolite ratios.

By way of reference, a non-tumoral tissue contribution to the spectra was analyzed on mice bearing subcutaneously implanted synthetic spheres ranging from 9 to 200 mm^2. The minimum size without a significant NMR signal was found to be a 'tumor area' of 25 mm^2. The skin overlying the tumor gave no detectable NMR signal under the acquisition conditions present.

The tumors were put out of the solenoid coil, where the induced radio frequency field was irregular. Field plots were obtained by using a sample of a 10 mM Pi solution in a capillary tube. With this small (10 mm diameter) coil and short duration pulses we were able to exclude non-tumoral tissue contamination from the spectra. As we used the same acquisition parameters for the large tumors, only their superficial part (3 mm layer) was analyzed.

8. *Steroid hormone receptor assays*

Estrogen (ER) and progesterone (PgR) receptors were measured on five 6-week-old MXT tumors borne by an additional group of intact mice. ER and PgR were assayed on cytosol preparations of the tumors according to the traditional dextran-coated charcoal method [33, 34]. The cytosol binding capacity for [^{3}H]E2 and [^{3}H]ORG2058 was expressed in femtomoles per milligram of protein.

9. *Statistical analyses*

Statistical comparisons of means were performed by using the Kruskal–Wallis test. ANOVA analyses of data were not permitted because of the too high variability of the data variances as revealed by the Bartlett test. Rank correlation between ratios and tumor areas was explored using the Spearman test.

RESULTS

1. *Histopathology, steroid receptor content and tumor growth*

All the MXT tumors, i.e. those borne by the OO and/or the CPA and/or the E2 + CPA treated mice, were poorly differentiated adenocarcinomas, whose peripheries showed small intermingled glandular elements, poorly differentiated polygonal cells and large centrum foci of necrosis [28].

CPA treatment significantly slowed down this growth from the 5th week post implantation (Fig. 1). The combined and sequential administration of E2 24 h prior to CPA completely abolished the CPA-induced effects (Fig. 1).

2. In vivo *and* in vitro ^{31}P *spectroscopy*

a. In vitro *spectra.* The proton coupled ^{31}P NMR spectrum of the MXT tumor extract is shown in Fig. 2. The region of the spectrum downfield of inorganic phosphate (Pi) at +2.73 ppm (peak 3) originates from phosphomonoesters: phosphoryl ethanolamine (PE) at +4.00 ppm (peak 1) and

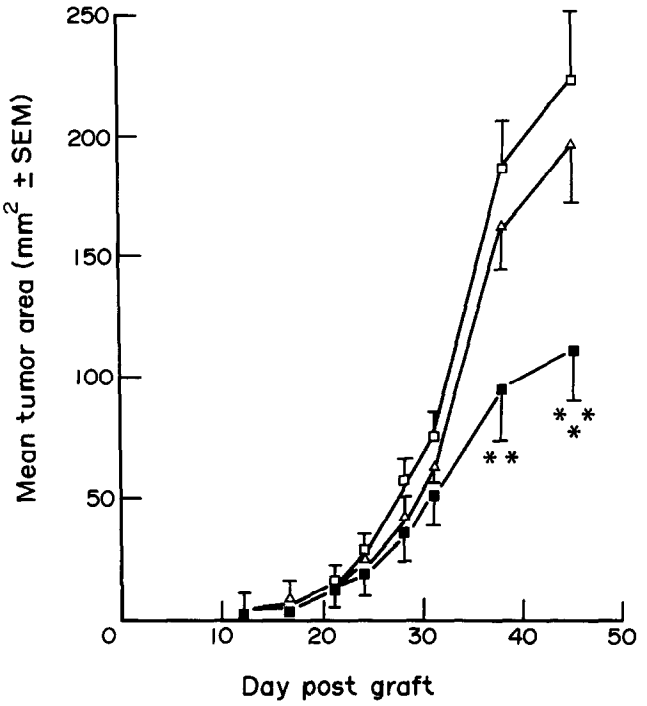

*Fig. 1. Growth pattern of the MXT mouse mammary tumor. Each value represents mean (± S.E.M. = bars) tumor size recorded in groups of 10 tumors. Fifteen days after transplantation all the animals, i.e. those belonging to groups OO (□), OO + CPA (△) and OO + E2 + CPA (■), were oophorectomized. In addition OO + CPA and OO + E2 + CPA groups received seven administrations of 20 mg/kg cyclophosphamide (CPA), every 2 days, from the 15th to the 27th day post-graft. Finally, animals belonging to the OO + E2 + CPA group were injected with 0.25 μg of 17-beta-estradiol (E2) 24 h prior to each CPA administration so that an attempt of estrogenic cell recruitment could be performed. The mean values (± S.E.M.) of tumor size in the OO + CPA and OO + E2 + CPA groups were statistically compared (Kruskal–Wallis test) to the control value (OO group) recorded at the same time (**P < 0.01; ***P < 0.001).*

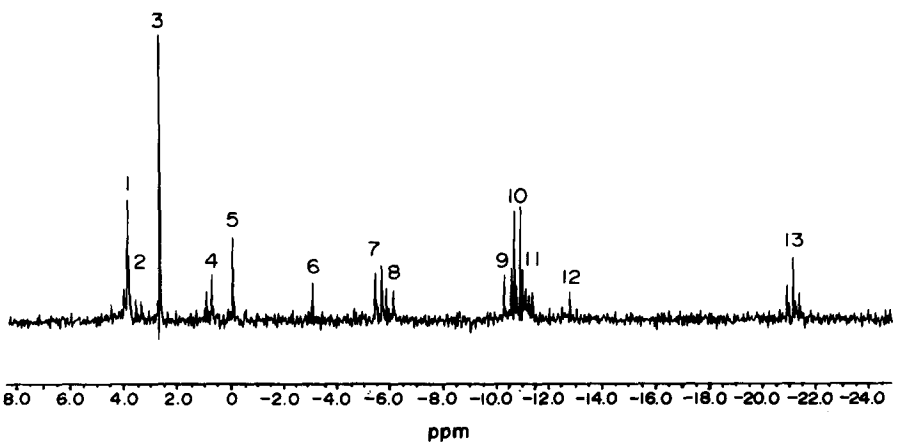

Fig. 2. Proton coupled ^{31}P NMR spectrum of a perchloric extract of 10 MXT tumors (OO group). Spectral conditions are: 8 k data ponts, 60° flip angle, + 2500 Hz sweep width, 2048 scans, 0.819 s repetition rate. Spectral assignments are: peak 1 = PE, phosphorylethanolamine; peak 2 = PC, phosphorylcholine; peak 3 = Pi, inorganic phosphate; peak 4 = GPE, glycerophosphorylethanolamine; peak 5 = GPC, glycerophosphorylcholine; peak 6 = PCr, phosphocreatine; peak 7 = gNTP, g-nucleoside triphosphate; peak 8 = bNDP, b-nucleoside diphosphate; peak 9 = aNDP, a-nucleoside diphosphate; peak 10 = aNTP, a-nucleoside triphosphate; peak 11 = NAD, nicotinamide; peak 12 = DPDE, diphosphodiesters; peak 13 = bNTP, b-nucleoside triphosphate.

phosphorylcholine (PC) at 3.60 ppm (peak 2). With regard to the ^{31}P NMR spectra extract, the PC peak is much less pronounced than the PE one, whereas glycerophosphorylcholine (GPC) at 0.00 ppm (reference, peak 5) appears more intense than glycerophosphorylethanolamine (GPE) at 0.79 ppm (peak 4). The sharp resonance at −3.00 ppm represents phosphocreatine (PCr, peak 6). The resonances centered at −5.47 ppm (doublet, peak 7), −10.63 ppm (doublet, peak 10), and −21.16 ppm (triplet peak 13) arise from gamma, alpha, and beta nucleoside triphosphate (NTP) respectively. The doublets at −10.34 ppm (peak 9) and −5.90 ppm (peak 8) originate respectively from alpha and beta nucleoside diphosphate (NDP) resonances. The NAD peak yields complex multiplets centered at −11.00 ppm (peak 11). Finally, the −12.71 ppm resonance (peak 12) is generally attributed to diphosphodiesters.

b. In vivo *spectra*. A representative *in vivo* spectrum from an MXT tumor borne by an oophorectomized animal (Fig. 3) was recorded on the 30th day post-graft. This spectrum illustrates the signal-to-noise ratio typically encountered in the present experimental conditions. Downfield of Pi at +2.05 ppm, the phosphomonoester region exhibited only one peak at +3.98 ppm assigned to PME. The GPC peak is taken as a chemical shift reference in Fig. 3. Higher PCr levels than those found in extracted materials were observed in the *in vivo* spectrum. At this stage of growth the tumor had reached 150 mm^2 and no spurious muscle signal could be incriminated. The high-energy part of the spectrum reported three well-defined resonances at −5.40 ppm (bATP + bADP), −10.51 ppm (aATP + aADP + NAD) and −1.92 ppm (bATP), respectively. The small resonance observed at −12.1 ppm was tentatively assigned to DPDE.

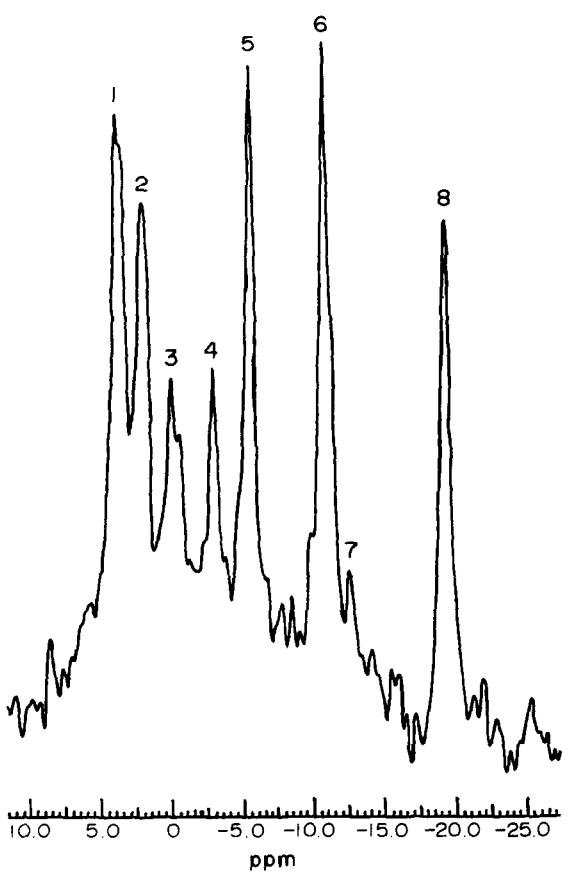

Fig. 3. Characteristic in vivo *spectrum of a metabolically active MXT tumor at the 30th day post-graft (OO group). The spectrum was obtained using approximate Ernst angle conditions with a* 60° *pulse width set at* 25 μs *and a* 3 s *repetition rate. The sweep width was* + 25500 Hz *with quadrature detection.* 600 *acquisitions were averaged. A* 15 Hz *line broadening filter was used. Spectral assignments were as follows*: 1: *PME at* +3.98 ppm; 2: *Pi at* +2.05 ppm; 3: *GPC (reference)*; 4: *PCr*; 5: *bATP + bADP*; 6: *aATP + aADP + NAD*; 7: *DPDE*; 8: *bATP*.

c. *Hormonotherapy-induced effects versus chemotherapy-induced effects on high energy* ^{31}P *NMR metabolites*. According to the Pi chemical shift used as a pH index [35], all the tumors exhibited an acidotic status (6.82 ± 0.21, pH units). The Pi chemical shifts were converted into pH units using laboratory calibration curves (data not shown) according to the following formula: pH = 6.76 − 0.38 log ((5.67 − Pi shift)/(Pi shift − 3.48)).

The acidotic status increased over time with no significant differences appearing between groups (Fig. 4), while there was an identical decrease in the intracellular pH index following tumor growth in all the experimental groups.

Several authors using high-dose chemotherapy (150–200 mg/kg CPA) have previously reported that significant effects may occur on neoplastic bioenergetics before any growth [31] or histopathological [35] modifications are observed. In order to test whether such a phenomenon might occur in an MXT model, we used low-dose chemotherapy by way of contrast and we divided our spectral population into two approximately equal groups: we chose a 120 mm^2 tumor area, corresponding to the 35th day post-graft, as a cut-off value between the two groups defined respectively as G1 (tumor size less than 120 mm^2) and G2 (tumor size equal to or larger than 120 mm^2). No statistically significant growth size differences appeared between the OO (69 + 5 mm^2), CPA (69 + 4 mm^2) and E2 + CPA (71 + 5 mm^2) mean values in G1.

Detectable ^{31}P NMR phosphate metabolite levels relating to bATP were modified along with increasing tumor volume: Pi and PME increased and PCr decreased. The bATP/PCr and Pi/PCr ratios had increased significantly for all the groups when we compared the small and the large tumors (Fig. 5). Figure 6 illustrates these modifications on a series of spectra acquired from the same MXT tumor grafted on to a CPA treated animal during tumor growth.

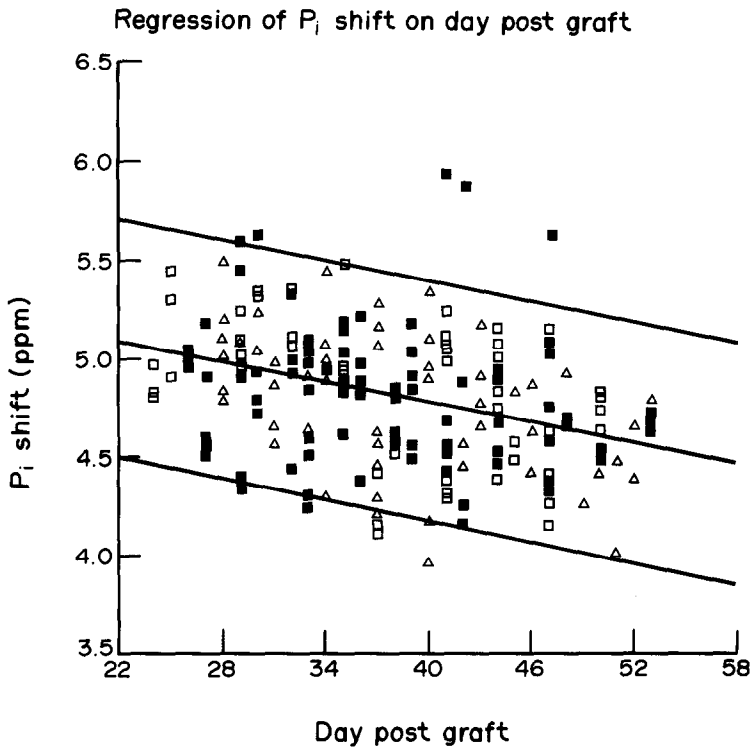

Fig. 4. Overall analysis of the chemical shifts in the inorganic phosphate (Pi) [with reference to phosphocreatine (PCr) peak in ppm] versus day post-graft (DPG). Simple linear regression: y = ax + b, *with* a = 5.48, b = 0.018 *and* r = −0.39. *There is a decrease in the intracellular pH index as a function of tumor growth and this decrease seems to be identical in the three experimental groups* (□ = *OO*; ■ = *OO + CPA*; △ = *OO + E2 + CPA*).

Possible changes in ^{31}P metabolite bioenergetics due to chemo- or hormonochemotherapy schedules were analyzed by a comparison (Kruskal–Wallis test) of the CPA or E2 + CPA group mean values, with those obtained in the OO group taken as reference. Data in Table 1A show that the mean OO group values are higher than those recorded in the CPA or E2 + CPA ones, a factor which suggests a lower amount of PCr in MXT OO-bearing tumor mice than in CPA- or E2 + CPA-bearing tumor animals, with the bATP being taken as invariant.

No significant differences appeared for the Pi/bATP ratio (not shown), a fact that would indicate a similar mean Pi retention across these three groups. It thus seems that it is the variation of the PCr level which could represent the variant element within the groups. Since the mean values in the CPA group were lower than those of the E2 + CPA group (Table 1A) estradiol seemed to antagonize the CPA-induced influence on the NMR ratios.

In addition to the data presented in Table 1, rank correlation analyses using the Spearman test showed that both bATP/PCr and Pi/PCr were highly correlated ($P < 0.001$) to the tumor area, a result suggesting that PCr might be involved in such correlations.

PME/bATP and PDE/bATP did not differ ($P > 0.05$) across the experimental groups (data not shown), whilst the PME/PDE ratio was lower in the OO + CPA group than in the OO one.

Table 1B illustrates the comparisons (Kruskal–Wallis test) of metabolic parameters performed on the treated experimental groups within G1. The mean ratios of the three groups (OO, OO + CPA and OO + E2 + CPA) showed the same trends as did the overall analysis. Although no significant differences appeared between the mean growth size values (Fig. 1), the hormonochemo- (OO + E2 + CPA) and chemotherapeutically (OO + CPA) treated tumors exhibited a higher bioenergetic status than the hormonotherapeutically (OO) treated ones, with the PCr level being higher in the OO + CPA and OO + E2 +CPA groups than in the OO group (Table 1B). Moreover, the results obtained in the OO + E2 + CPA group were less pronounced than those of the OO + CPA group (Table 1B).

Within the G2 group, made up of animals bearing tumors larger than or equal to 120 mm^2, the OO + CPA group (162 ± 9 mm^2) had a significantly ($P > 0.01$) lower mean tumor size in comparison with the OO (209 ± 13 mm^2) or

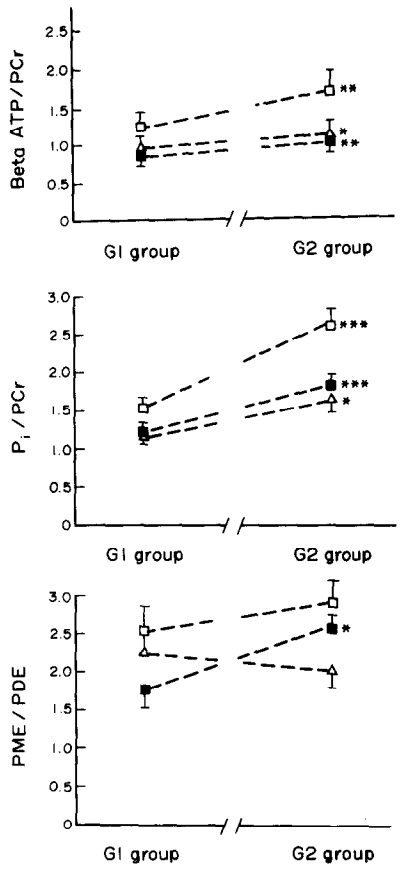

Fig. 5. Plot of phosphate metabolites (mean ± S.E.M.) for the three experimental groups (OO = □, OO + CPA = ■ and OO + E2 + CPA = △) divided into 'tumors smaller than 120 mm^2*' (G1 sub-group) and 'tumors equal to or larger than* 120 mm^2*' (G2 sub-group). The mean value ± S.E.M. of the G2 group was statistically compared (Kruskal–Wallis test) to the corresponding value of the G1 group* (*P < 0.05; **P < 0.01; ***P < 0.001).

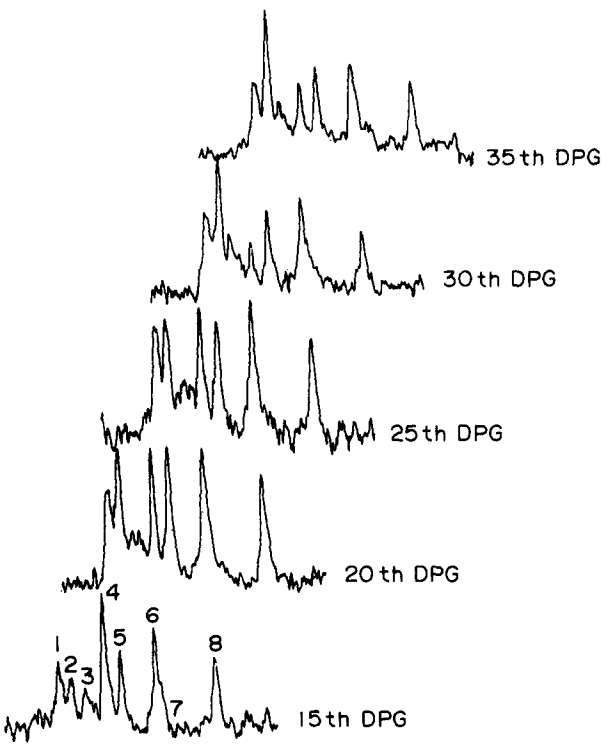

Fig. 6. Series of MXT ^{31}P spectra (CPA treated mouse) showing NMR modification along growth (15th DPG to 35th DPG). There is an increase of bATP/PCr and of Pi/PCr. Resonance assignments are those of Fig. 3.

OO + E2 + CPA (199 ± 11 mm^2) groups.

bATP/PCr and Pi/PCr were found to be significantly different in the OO + CPA and OO + E2 + CPA group as compared to the OO group (Table 1C).

DISCUSSION

As argued by Davidson and Lippman [36], breast cancer treatment has been the subject of intense investigation with regard to hormonal and/or chemotherapeutic approaches. These authors nevertheless state that only 40–70% of patients will respond to first-line multi-drug regimens, and these patients will have a median survival of 12–24 months; in an unselected patient population about 35% to endocrine therapy. Endocrine therapy consists of the removal of endogeneous estrogen via ablative or chemical procedures, or of the blocking of the estrogen effects by antiestrogen administration [2, 5–11]. Cytotoxic drugs are recommended for patients whose tumors are unlikely to respond to endocrine therapy [2, 23]. Some experimental data have shown that while neither endocrine, i.e. estradiol (E2), nor cytotoxic, i.e. cyclophosphamide (CPA), drugs alone inhibit tumor growth, these two kinds of compounds may be synergistic and may block the growth of experimental mammary tumors such as the MXT mouse model, for instance [23, 24].

In our present experiments we used such a combined endocrine/chemotherapeutic regimen on the MXT mammary tumor in order to detect by ^{31}P nuclear magnetic resonance (NMR) the eventual positive therapeutic effects that might occur prior to any macroscopic modifications. We chose a borderline hormone-sensitive MXT strain to study a 'clinically' relevant reality, i.e. a mammary tumor with an ER + PgR − 'phenotype' and a poorly differentiated histopathological pattern since this kind of breast neoplasm represents 50% of the cases unresponsive to hormone therapy out of the 80% ER positive cases [2].

We conducted our experiment to evaluate the remaining 'long-term' modifications induced by CPA treatment rather than the direct cytotoxic effect. Indeed, NMR measurements only began at the end of the CPA administration and not during this treatment, as was the case in our preliminary study [25].

The results relative to MXT growth curves indicated that this mammary tumor was able to grow on oophorectomized mice and we observed no differ-

Table 1. Effects after treatment schedules on NMR parameters

NMR ratios	OO[a]	OO + CPA	OO + E2 + CPA
A. Data analyses of the whole population[b]			
bATP/PCr	1.37 ± 0.08	0.91 ± 0.04[c]	1.00 ± 0.05[d]
		***	*
Pi/PCr	1.99 ± 0.16	1.49 ± 0.11	1.54 ± 0.11
		***	**
PME/PDE	2.74 ± 0.17	2.06 ± 0.11	2.26 ± 0.11
		***	*
B. Data analyses of tumors <120 mm²[e]			
bATP/PCr	1.23 ± 0.07	0.85 ± 0.05	0.94 ± 0.06
		***	*
Pi/PCr	1.51 ± 0.15	1.29 ± 0.15	1.36 ± 0.18
		*	n.s.
PME/PDE	2.49 ± 0.20	1.84 ± 0.13	2.28 ± 0.19
		*	n.s.
C. Data analyses on tumors >120 mm²[f]			
bATP/PCr	1.50 ± 0.14	1.01 ± 0.06	1.05 ± 0.12
		**	*
Pi/PCr	2.44 ± 0.26	1.87 ± 0.12	1.69 ± 0.13
		*	**
PME/PDE	2.97 ± 0.26	2.44 ± 0.19	2.19 ± 0.12
		n.s.	n.s.

[a]OO = ovariectomized animals; CPA = chemotherapy with cyclophosphamide; E2 = attempt at cell recruitment by 17-beta-estradiol prior to each CPA administration.
[b]OO: $n = 56$; OO + CPA: $n = 67$; OO + E2 + CPA: $n = 63$ measurements.
[c]Mean ± S.E.M.
[d]Statistical significance versus the OO group by Kruskal–Wallis test: n.s. = $P > 0.05$; *$P < 0.05$; **$P < 0.01$; ***$P < 0.001$.
[e]OO: $n = 21$; OO + CPA: $n = 38$; OO + E2 + CPA: $n = 23$ measurements.
[f]OO: $n = 35$; OO + CPA: $n = 29$; OO + E2 + CPA: $n = 40$.

ences between the growth curves of MXT tumors grafted onto intact, i.e. non-ovariectomized, animals and those of tumors grafted onto ovariectomized mice (data not shown). This apparent absence of MXT growth sensitivity to oophorectomy leads us to suggest that the strain used here was hormone sensitive (HS) rather than hormone dependent (HD). In fact, we can exclude the possibility that these neoplasms were hormone independent (HI) by referring both to the presence of low but nevertheless significant amounts of ER and to the results, obtained in the OO + E2 + CPA group, which showed a clear-cut antagonistic effect of E2 versus CPA on MTX growth. This HS property of the MXT model has been previously described [28] and might correspond to the natural evolution from an HD to an HI stage, a phenomenon well documented in the literature on murine mammary tumors [12, 28, 37, 38].

The present lack of a synergistic effect between the combined chemoendocrine therapy, i.e. the expected E2–CPA co-operativity, has been reported on several previous occasions (for review see [36]). It might now be explained by an E2-induced mitogenic response exceeding 24 h, i.e. of 36 or 48 h duration, because of the fact that E2 exerts a transient effect on an MXT tumor that this generally occurs at a maximum of 24 h after its administration to the bearing animal, but only with significant 'tail' effect that may remain present until the 36th or 48th h post-injection [16–18, 20, 21].

Progressive changes in phosphate tumor metabolites occurring during growth were assessed through the following bioenergetic ratios: bATP/PCr, bATP/Pi and Pi/PCr, whereas PME/bATP, PDE/bATP and PME/PDE reflect metabolism of the phospholipids. The values of our spectral assignments corroborated well with those found in other murine tumors like radiation-induced fibrosarcoma [30] or NU-82 mammary carcinoma [29]. We found that in all the groups, the bATP/PCr and Pi/PCr ratios increased during tumor growth whereas the

pH value decreased. Moreover, the sudden decrease in high-energetic phosphates and the concomitant increase in inorganic phosphates could be due to progressive hypoxia [39]. We obtained a pH value of 6.8 in the MXT tumor in agreement with Vaupel *et al.* [40], who observed that C3H mouse mammary adenocarcinoma contain a high level of tissular acidosis represented by a mean pH value of 6.73. It must be remembered that the normal tissue pH value varies from 7.3 to 7.4 [40]. These authors also report that in human mammary tumors grafted onto nude rats, an increase of oxygen metabolism correlates with a decrease [40] in tumoral blood flow. In our experimental model, the gradual decrease in high-energetic compounds, mainly PCr, could be explained by a decrease in oxygen available due to the gradual damage of microvascularization concomitant with an increase in the energy requirement involved in cell proliferation. Likewise, the progressive PCr decrease (with bATP being invariant) might be due to a progressive decrease in spectral contamination induced by a non-tumoral muscular signal. We also show that E2 treatment slows down the significant PCr decrease since our OO + E2 + CPA group contained a higher value than the OO + CPA one.

When we compared the G1 group (small tumors: mean tumoral area <120 mm^2) with G2 (large tumors: mean tumoral area >120 mm^3), it appeared that only the small tumors treated with CPA contained significantly more PCr and that the PME/PDE ratio stayed lower than in the OO or OO +E2 + CPA G1 groups; this fact is in good agreement with the growth-inhibitory effect induced by CPA (*cf.* growth curves). In the large tumors, i.e. the G2 group, it seemed that the necrotic fraction extent could mask any effect. Thus, when no macroscopic effects were detectable, the better PCr preservation could be explained by a decrease in the energy requirement concomitant with a decrease in cell proliferation. This is in good agreement with Rodriguez *et al.* [41] who observed that ovariectomy performed on mice grafted with estrogen sensitive mammary tumors, induced a PCr increase. The non significant effect across the OO + E2 + CPA and OO + CPA G2 groups was due to the complexity of the biological phenomenon. In fact, we suppose that the OO + E2 + CPA tumors could show the stimulating effect of the estrogen-sensitive fraction concomitantly with the slowing down effect of the chemosensitive one.

Methodological limitations could also be involved in the present results since we performed relatively few measurements and since the analyses, limited as they were to spectra–intensity ratios, avoided any real metabolite quantification.

Concerning the phospholipid data, only the dosage of the PME/PDE ratio was significant in the groups treated; this is probably due to the PME decrease and the PDE increase induced by chemotherapy. Since, in the ^{31}P NMR *in vitro* and *in vivo* experiments the phosphomonoester level was higher in non-proliferative tissues, this parameter is proposed as a tumor marker [4, 26]. Bearing in mind that PME and PDE are involved in phospholipid metabolism, Maris *et al.* [42] report that PME/bATP decreases as a function of therapeutic efficiency in a human neuroblastoma. Proietti *et al.* [43] also describe the decrease in phosphorylcholine in interferon-treated Friend erythroleukemia cells.

The phospholipid precursors were difficult to analyze due to the fact that the peaks overlapped. Also, the efficiency of the deconvolution analysis software was sometimes impaired by the low signal-to-noise ratio of the *in vivo* spectra. Nevertheless, lower PME/PDE values in the G1 OO + CPA group in comparison with the G1 OO one support the hypothesis that a decrease in this ratio might represent a good indicator of an efficient therapeutic influence. However, we should underline the fact that the great variability in measurements in this part of the spectrum reflects day-to-day biological modifications and analysis limitations, and could dramatically impair the value of the test if only small spectra series are considered. The wide variability of our spectra probably resulted from the therapeutic and biological complexity of the model used. In a multinuclear NMR study performed on an R3250AC mammary adenocarcinoma transplanted into rats, Block *et al.* [44] show that estrogen treatment induces a relative decrease in the PCr/bATP ratio.

As revealed by the growth curves, Pi accumulation could be explained by the fact that the damaged cells are not eliminated. Concerning Pi evolution, its accumulation could explain why the damaged cells are not eliminated, as is suggested by the growth curves. In a previous work [25], we showed that an MXT tumor treated on a similar schedule showed higher hypoxia in the treated tumor in comparison with the control ones. When the growth curves displayed the same profile, the Pi/PCr ratio increase could be due to Pi accumulation in the damaged cells of the treated tumors. It must be remembered that the measurements were consistent during the treatment and not after, in the present case. We could hypothetize that, in the present work, we have observed the cytocidal effect induced by the treatment alone.

The non-invasive follow-up of treatment is probably the most interesting potentiality of *in vivo* ^{31}P NMR for the management of cancerous patients. The present methodology, which is not capable of undergoing bioenergetic compound quantification, enables us to show statistically significant differences in the phospholipidic and energy metabolisms

between the two chemo- or hormonochemotreated groups and the control one. Since the sense and magnitude of the response seem to be different according to the experimental model, the treatment and/or the duration of the experiments, we should beware of possible future extrapolations of our results to other tumor models and to other kinds of treatment. Nevertheless, together with preliminary human tumor measurements using surface coils [45, 46], the recent technical improvement in *in vivo* NMR high-field units (1.5–2.0 T) for localized ^{31}P spectroscopy phase-encoding methods [47, 48] may indicate that this technique could be used for patients. Furthermore, the monitoring procedure might be improved by experimental data. Concerning the latter, many publications already exist [26, 27] which report high-dose chemotherapeutic effects, but which have a low degree of relevance from a clinical point of view. Be this as it may, the present work reinforces the hypothesis that the metabolic data of *in vivo* spectra could be used with other techniques such as *in vivo* anticancer therapeutic markers.

Acknowledgements—We wish to thank C. Maerschalk and Mr. S. Gras for their excellent technical assistance. This work is supported by grants awarded by the 'Fonds de la Recherche Scientifique Médicale' (FRSM: no 3.45.69.87) and by the 'Institut pour l'encouragement de la Recherche Scientifique dans l'Industrie et l'Agriculture' (IRSIA), Belgium.

REFERENCES

1. Beatson, GT. On the treatment of inoperable cases of carcinoma of the mamma. Suggestion for a new method of treatment with illustrative cases. *Lancet* 1896, **2**, 104–107.
2. Paridaens RJ, Leclercq G, Piccart MJ, Kiss R, Mattheiem WH, Heuson JC. Comments on the treatment of breast cancer. *Cancer Surv* 1986, **5**, 447–461.
3. Jensen EV, Suzuki T, Kawashima T, Stumpf WE, Jungblut PW, De Sombre ER. A two-step mechanism for the interaction of estradiol with rat uterus. *Proc Natl Acad Sci USA* 1968, **59**, 632–638.
4. Korenman SG. Specific estrogen binding by the cytoplasm of human breast carcinoma. *J Clin Endocrinol* 1970, **30**, 639–645.
5. McGuire WL, Vollmer EP, eds. *Estrogen Receptors in Human Breast Cancer*. Raven Press, New York, 1975.
6. Jensen EV. Hormone dependency of breast cancer. *Cancer* 1981, **47**, 2319–2326.
7. Paridaens R, Sylvester R, Ferrazzi E, Legros N, Leclercq G, Heuson JC. Clinical significance of the quantitative assessment of estrogen receptors in advanced breast cancer. *Cancer* 1980, **46**, 2889–2895.
8. Santen RJ, Brodie AMH. Suppression of estrogen production as treatment of breast carcinoma: pharmacological and clinical studies with aromatase inhibitors. In: Furr BJA, ed. *Hormone Therapy—Clinics in Oncology*. London, WB Saunders, 1982, Vol. 1, 77–130.
9. Goss E, Bowles TJ, Dowsett M *et al.* Treatment of advanced postmenopausal breast cancer with an aromatase inhibitor, 4-hydroxyandrostenedione: phase II report. *Cancer Res* 1986, **46**, 4823–4826.
10. Bradbeer JW, Kyngdon J. Primary treatment of breast cancer in the elderly women with tamoxifen. *Clin Oncol* 1983, **9**, 31–34.
11. McGuire WL, Clark GM, Dressler LG, Owens MA. Role of steroid hormone receptors in prognostic factors in primary breast cancer. *NCI Monogr* 1986, **1**, 19–23.
12. Briand P. Hormone-dependent mammary tumors in mice and rats as a model for human breast cancer (review). *Anticancer Res* 1983, **3**, 273–282.
13. Watson CS, Medina D, Clark JH. Estrogen receptor characterization in a transplantable mouse mammary tumor. *Cancer Res* 1977, **37**, 3344–3348.
14. Watson CS, Medina D, Clark JH. Characterization and estrogen stimulation of cytoplasmic progesterone receptor in the ovarian-dependent MXT-3590 mammary tumor line. *Cancer Res* 1979, **39**, 4098–4104.
15. Watson CS, Medina D, Clark JH. Estrogenic effects of Nafoxidine on ovarian-dependent and independent mammary tumor lines in the mouse. *Endocrinology* 1981, **108**, 668–672.
16. Paridaens RJ, Danguy AJ, Leclercq G, Kiss R, Heuson JC. Effect of castration and 17-beta-estradiol pulse on cell proliferation in the uterus and the MXT mouse mammary tumor. *J Natl Cancer Inst* 1985, **74**, 1239–1246.
17. Kiss R, Paridaens R, Leclercq G, Danguy A. Sensitivity of the hormone dependent MXT-mouse mammary carcinoma to estradiol during tumoral growth. An autoradiographic study. *Eur J Cancer Clin Oncol* 1986, **22**, 849–856.
18. Kiss R, Danguy A, Heuson JC, Paridaens R. Effect of estradiol on proliferation and cell loss in the MXT mouse mammary tumor. *Anticancer Res* 1986, **6**, 1321–1328.
19. Kiss R, Paridaens RJ, Heuson JC, Danguy A. Effect of progesterone on cell proliferation in the MXT mouse hormone-sensitive mammary neoplasm. *J Natl Cancer Inst* 1986, **77**, 173–178.
20. Kiss R, Danguy A, Heuson JC, Paridaens RJ. Synergism or antagonism between estradiol and progesterone on the cell kinetic parameters of the MXT mouse mammary tumor. *J Natl Cancer Inst* 1987, **78**, 573–579.
21. Kiss R, de Launoit Y, L'Hermite-Balériaux M *et al.* Effect of prolactin and estradiol on cell proliferation in the uterus and the MXT mouse mammary neoplasm. *J Natl Cancer Inst*

1987, **78**, 993–998.
22. de Launoit Y, Kiss R, Danguy A, Paridaens R. Effect of ovariectomy, hypophysectomy and/or GnRH analog (HRF) administration on the cell proliferation of the MXT mouse hormone-dependent mammary tumor. *Eur J Cancer Clin Oncol* 1987, **23**, 1443–1430.
23. Markaveritch BM, Medina D, Clark JH. Effects of combination estrogen:cyclophosphamide treatment on the growth of the MXT transplantable mammary tumor in the mouse. *Cancer Res* 1983, **43**, 3208–3211.
24. Paridaens RJ, Kiss R, de Launoit Y *et al.* Chemotherapy with estrogenic recruitment in breast cancer: experimental and clinical studies. In: Klijn JGM, Paridaens RJ, Foekens JA, eds. *Hormonal Manipulation of Cancer. Peptides, Growth Factors and New (Anti) Steroidal Agents*. Raven Press, Monograph Series of the EORTC, 1987, Vol. 18, 477–486.
25. Scheiber C, Kiss R, de Launoit Y, Frühling J. MXT mammary tumor treated by low dose chemotherapy. A ^{31}P NMR and ^{1}H MRI study. *Anticancer Res* 1988, **8**, 403–408.
26. Evanochko WT, Ng TC, Glickson JD. Application of *in vivo* NMR spectroscopy to cancer. *Magn Reson Med* 1984, **1**, 508–534.
27. Sostman HD, Armitage IM, Fisher JJ. NMR in cancer. 1. High resolution spectroscopy of tumors. *Magn Reson Imaging* 1984, **2**, 265–278.
28. Danguy AJ, Kiss R, Leclercq G, Heuson JC, Pasteels JL. Morphology of MXT mouse mammary tumors. Correlation with growth characteristics and hormone sensitivity. *Eur J Cancer Clin Oncol* 1986, **22**, 69–75.
29. Sijens PE, Bovee WMMJ, Seijkens D, Los G, Rutgers DH. *In vivo* ^{31}P nuclear magnetic resonance study of the response of a murine mammary tumor to different doses of gamma-radiation. *Cancer Res* 1986, **46**, 1427–1432.
30. Evanochko WT, Sakai T, Ng TC *et al.* NMR study of *in vivo* RIF-1 tumors: analysis of perchloric acid extracts and identification of ^{1}H, ^{31}P and ^{13}C resonances. *Biochem Biophys Acta* 1984, **805**, 104–116.
31. Ng TC, Evanochko WT, Hiramoto RN *et al.* ^{31}P NMR spectroscopy of *in vivo* tumors. *J Magn Reson* 1982, **49**, 271–286.
32. Gordon RE, Timms WE. An improved time and match circuit for BO shimming in intact biological samples. *J Magn Reson* 1982, **46**, 322–324.
33. EORTC Group. Revision of the standards for the assessment of hormone receptors in human breast cancer. *Eur J Cancer Clin Oncol* 1980, **16**, 1513–1515.
34. Duffy MJ, Duffy GJ. Studies on progesterone receptors in human breast carcinomas: use of natural and synthetic ligands. *Eur J Cancer Clin Oncol* 1979, **15**, 1181–1184.
35. Roberts JK, Wade-Jardetzky N, Jardetzky O. Intracellular pH measurements by ^{31}P nuclear magnetic resonance. Influence of factors other than pH on ^{31}P chemical shifts. *Biochemistry* 1981, **20**, 5389–5394.
36. Davidson NE, Lippman ME. Stimulation of breast cancer with estrogens: how much clinical value? *Eur J Cancer Clin Oncol* 1987, **23**, 897–900.
37. Sluyser M, Van Nie R. Estrogen receptor content and hormone-responsive growth of mouse mammary tumors. *Cancer Res* 1974, **34**, 3253–3257.
38. Briand P, Rose C, Thorpe SM. Spontaneous regrowth of regressed hormone dependent tumours after long periods of time. *Eur J Cancer Clin Oncol* 1982, **18**, 1391–1393.
39. Vaupel P, Frinak S, Bicher H. Heterogeneous oxygen partial pressure and pH distribution in C3H mouse mammary adenocarcinoma. *Cancer Res* 1981, **41**, 2008–2013.
40. Vaupel P, Fortmeyer HP, Runkel S, Kallinowski F. Blood flow, oxygen consumption and tissue oxygenation of human breast cancer xenograft in nude rats. *Cancer Res* 1987, **47**, 3496–3503.
41. Rodriguez LM, Midwood CJ, Coombes RC, Stevens AN, Stubbs M, Griffiths JR. ^{31}P nuclear magnetic resonance spectroscopy studies of the response of rat mammary tumors to endocrine therapy. *Cancer Res* 1988, **48**, 89–93.
42. Maris JM, Evans AE *et al.* ^{31}P nuclear magnetic resonance spectroscopic investigation of human neuroblastoma *in situ*. *N Engl J Med* 1985, **312**, 1500–1505.
43. Proietti E, Carpinelli G, Di Vito M, Bellardelli F, Gresser I, Podo F. ^{31}P nuclear magnetic resonance analysis of interferon-induced alterations of phospholipids metabolites in interferon-sensitive and interferon-resistant Friend leukemia cell tumors in mice. *Cancer Res* 1986, **46**, 2849–2857.
44. Block RE, Parekh B. Multinuclear magnetic resonance spectral studies of normal and tumor rat mammary tissues. *J Magn Res* 1987, **75**, 517–522.
45. Oberhaensli RD, Hilton-Jones D, Bore PJ, Rampling RP, Hands LJ, Radda GK. Biochemical investigation of human tumors *in vivo* with phosphorus-31 magnetic resonance spectroscopy. *Lancet* 1986, **ii**, 8–11.
46. Bottomley PA, Drayer BP, Smith LS. Chronic adult cerebral infarction studied by phosphorus NMR spectroscopy. *Radiology* 1986, **160**, 763–766.
47. Bailes DR, Bryant DJ, Bydder GM *et al.* Localized phosphorus-31 NMR spectroscopy of normal and pathological human organ *in vivo* using phase encoding techniques. *J Magn Reson* 1987, **74**, 158–170.
48. Segebarth C, Luyten PR, Den Hollander JA. Improved depth-selective single surface-coil ^{31}P NMR spectroscopy using a combination of B1 and B0 selection techniques. *J Magn Reson* 1987, **75**, 345–351.